Functional Characterization of the Subunits N, H, J, and O of the NAD(P)H Dehydrogenase Complexes in *Synechocystis* sp. Strain PCC 6803[1][OPEN]

Zhihui He and Hualing Mi*

National Key Laboratory of Plant Molecular Genetics, Institute of Plant Physiology and Ecology, Shanghai Institutes for Biological Sciences, Chinese Academy of Science, Shanghai 200032, China

ORCID IDs: 0000-0003-4184-8377 (Z.H.); 0000-0003-1021-8372 (H.M.).

The cyanobacterial NAD(P)H dehydrogenase (NDH-1) complexes play crucial roles in variety of bioenergetic reactions such as respiration, CO_2 uptake, and cyclic electron transport around PSI. Recently, substantial progress has been made in identifying the composition of subunits of NDH-1 complexes. However, the localization and the physiological roles of several subunits in cyanobacteria are not fully understood. Here, by constructing fully segregated *ndhN*, *ndhO*, *ndhH*, and *ndhJ* null mutants in *Synechocystis* sp. strain PCC 6803, we found that deletion of *ndhN*, *ndhH*, or *ndhJ* but not *ndhO* severely impaired the accumulation of the hydrophilic subunits of the NDH-1 in the thylakoid membrane, resulting in disassembly of NDH-1MS, NDH-1MS′, as well as NDH-1L, finally causing the severe growth suppression phenotype. In contrast, deletion of NdhO affected the growth at pH 6.5 in air. In the cytoplasm, either NdhH or NdhJ deleted mutant, but neither NdhN nor NdhO deleted mutant, failed to accumulate the NDH-1 assembly intermediate consisting of NdhH, NdhJ, NdhK, and NdhM. Based on these results, we suggest that NdhN, NdhH, and NdhJ are essential for the stability and the activities of NDH-1 complexes, while NdhO for NDH-1 functions under the condition of inorganic carbon limitation in *Synechocystis* sp. strain PCC 6803. We discuss the roles of these subunits and propose a new NDH-1 model.

Thylakoid membranes of cyanobacteria contain a NAD(P)H dehydrogenase (NDH-1) complex, homologous to complex I (NADH: ubiquinone oxidoreductase) from the mitochondria and eubacteria (Friedrich et al., 1995; Friedrich and Scheide, 2000). The NDH-1 complexes in cyanobacteria are involved in respiration and cyclic electron transport (CET) around PSI (Ogawa, 1991; Mi et al., 1992, 1995; Peltier and Cournac, 2002; Munekage et al., 2004). In addition, cyanobacterial NDH-1 complexes function in inorganic carbon concentrating mechanisms (Ogawa, 1991; Ohkawa et al., 2000).

In cyanobacteria, *ndhA-ndhK* encode proteins homologous to subunits of *Escherichia coli* complex I. However, homologous genes encoding the three subunits, NuoE-NuoG, constituting the catalytic domain of *E. coli* complex I, are not found in the genome of the cyanobacteria. There are six *ndhD* and three *ndhF* genes in *Synechocystis* sp. strain PCC 6803 (*Synechocystis* 6803). Different NDH-1 complexes consist of different types of NdhD and NdhF subunits, which are involved in diverse physiological functions. Four types of cyanobacterial NDH-1 complexes have been defined by reverse genetics (Klughammer et al., 1999; Shibata et al., 2001) and functional proteomics (Prommeenate et al., 2004; Battchikova et al., 2005). The large NDH-1 complex (NDH-1L) containing NdhD1/NdhF1 and the NDH-1L′ complex containing NdhD2/NdhF1 are involved in respiration and NDH-1 dependent CET around PSI (Ohkawa et al., 2000; Battchikova et al., 2011a). The expression of NDH-1L complex is stable under different growth conditions; however, the NDH-1L′ complex has not been detected on the protein level (Zhang et al., 2004).

All of these NDH-1 complexes contain a medium size NDH-1 complex (NDH-1M) as a skeleton. One type of NDH-1 complex, the NDH-1MS complex, is inducible at limiting inorganic carbon conditions and has a high uptake affinity for CO_2, which is easily dissociated into NDH-1M and a small size NDH-1 complex (NDH-1S; Herranen et al., 2004). The NDH-1MS complex has been isolated from a *Thermosynechococcus elongatus* strain in which the C terminus of NdhL has been tagged with 6-His. This complex is easily dissociated into NDH-1M and NDH-1S complexes (Zhang et al., 2005). NDH-1MS has been characterized as a U-shape structure by analysis of single-particle electron microscopy after purification from the thylakoid membranes of *T. elongatus* (Arteni et al., 2006). CupA is responsible for the U-shape

[1] This work was supported by funds from the State Key Basic Research and Development Plan 973 (2015CB150104 and 2013CB127005), the National Natural Science Foundation of China (31270286), and the Shanghai Science Foundation (13DJ1400102).

* Address correspondence to mihl@sippe.ac.cn.

The author responsible for distribution of materials integral to the findings presented in this article in accordance with the policy described in the Instructions for Authors (www.plantphysiol.org) is: Hualing Mi (mihl@sippe.ac.cn).

Z.H. and H.M. conceived and designed the experiments; Z.H. carried out all experiments and analyzed the data; Z.H. and H.M. wrote the article.

[OPEN] Articles can be viewed without a subscription.

www.plantphysiol.org/cgi/doi/10.1104/pp.16.00458

by binding at the tip of the membrane-bound arm of NDH-1MS in both *T. elongatus* and *Synechocystis* 6803 (Folea et al., 2008). As a homologous gene of *cupA*, *cupB* is involved in constitutive CO_2 uptake system and forms a small complex NDH-1S′ (Shibata et al., 2001; Maeda et al., 2002). It has been found that CupB protein is localized in thylakoid membrane but is absent in that of NdhD4 deleted mutant (Xu et al., 2008). Based on the result that the purification of a 450-kD complex contained both NdhH and CupB protein, it has been suggested that the complex is NDH-1MS′ located in the thylakoid membranes.

Four additional subunits (NdhL-NdhO) specific for cyanobacteria and chloroplasts have been identified in *Synechocystis* 6803 and Arabidopsis (*Arabidopsis thaliana*; Prommeenate et al., 2004; Battchikova et al., 2005; Rumeau et al., 2005; Shimizu et al., 2008). Further electron microscopy investigations speculated that in *Synechocystis* 6803, the NdhL-NdhO subunits are located together, constituting the oxygenic photosynthesis specific (OPS) domain (Birungi et al., 2010). However, our previous study demonstrates that cyanobacterial NdhM is localized in the hydrophilic subcomplex of NDH-1 complexes and is essential for the function of NDH-1 complexes (He et al., 2016). Nowaczyk et al. (2011) reported two novel small subunits, NdhP and NdhQ, which were included in the purified NDH-1L complex by Ni^{2+} affinity chromatography and size-exclusion chromatography from *T. elongatus*. Recently, it has been demonstrated that NdhP and NdhQ are involved in respiration and CET and are required to stabilize the NDH-1L complex (Schwarz et al., 2013; Wulfhorst et al., 2014; Zhang et al., 2014; Zhao et al., 2015). In recent years, it has been reported that the newly identified OPS subunit, NdhS from Arabidopsis (also known as CRR31) or from *Synechocystis* 6803 contains Src homology 3 domain-like fold, which serves as the ferredoxin (Fd) docking site domain (Yamamoto et al., 2011; Battchikova et al., 2011b; Yamamoto and Shikanai, 2013), and the authors suggested that the chloroplast NDH complex could accept electrons from Fd rather than NAD(P)H. By studying the purified NDH-1L complex from the thermophilic cyanobacterium *T. elongatus*, we demonstrated that NDH-1L

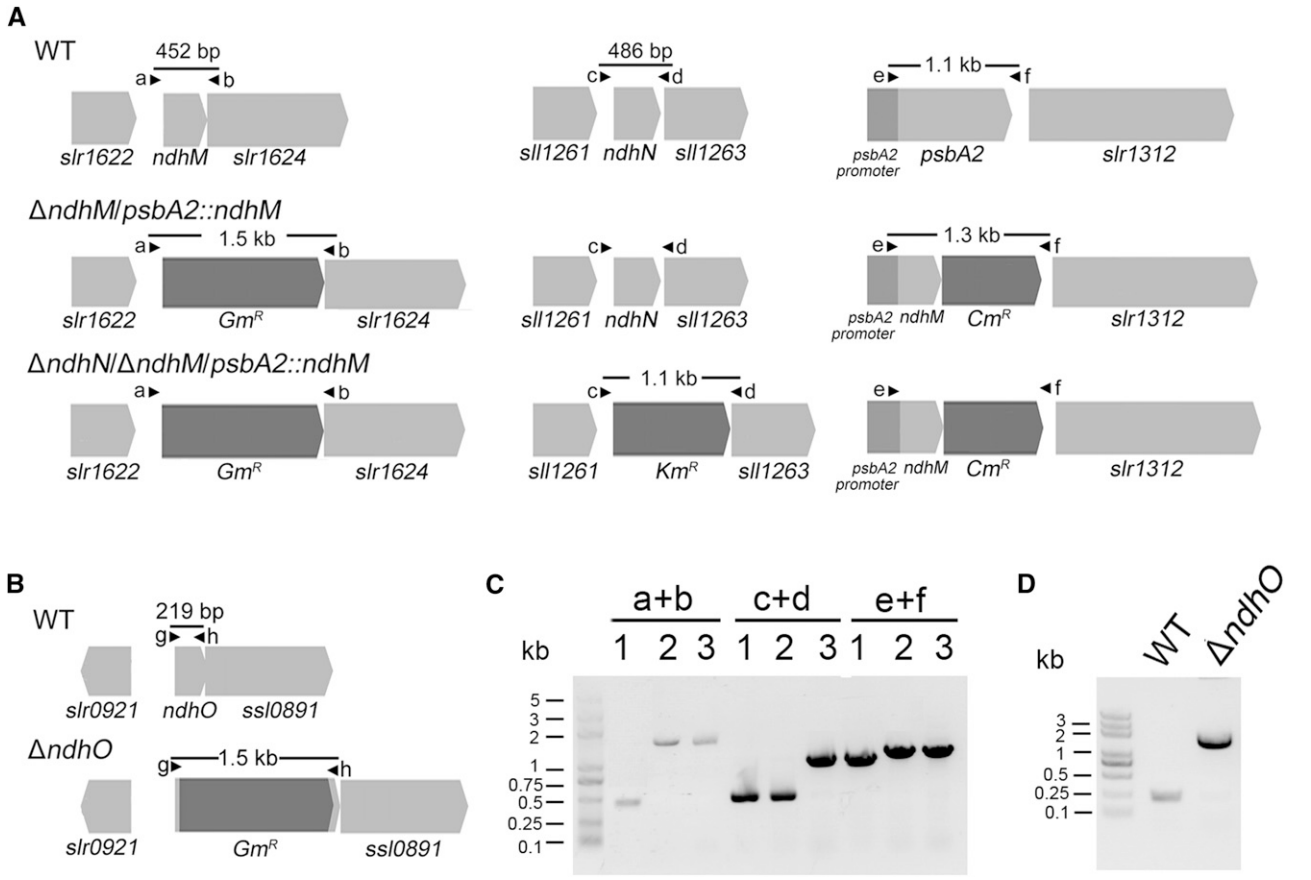

Figure 1. Construction and verification of the *ndhN*-deletion and *ndhO*-deletion mutants. A, Construction of the plasmids used to generate the Δ*ndhM*/*psbA2*::*ndhM* and Δ*ndhN*/Δ*ndhM*/*psbA2*::*ndhM*. B, Construction of the plasmid to generate the Δ*ndhO* construct. C and D, PCR segregation analysis of the Δ*ndhM*/*psbA2*::*ndhM*, Δ*ndhN*/Δ*ndhM*/*psbA2*::*ndhM*, and Δ*ndhO* mutants using the primers listed in Supplemental Table S1. Primer location is shown in A and B, and the expected DNA fragment size is based on the DNA template. 1, Wild type; 2, Δ*ndhM*/*psbA2*::*ndhM*; 3, Δ*ndhN*/Δ*ndhM*/*psbA2*::*ndhM*.

complex interacts with Fd via the subunit NdhS (He et al., 2015). Gao et al. (2016) identified the new NdhV subunit in *Synechocystis* 6803 and proposed that NdhV cooperates with NdhS to accept electrons from Fd. In addition, *ndhH* gene was shown to be vital to the survival of *Synechocystis* 6803 even under high-CO_2 growth conditions (Pieulle et al., 2000). NdhJ was found in both plasma membrane and thylakoid membranes in *Synechocystis* 6803 (Berger et al., 1991; Pieulle et al., 2000) and *Anacystis nidulans* (Dworsky et al., 1995). The NdhN and NdhO subunits of *Synechocystis* 6803 were first identified by functional proteomics approach (Prommeenate et al., 2004; Battchikova et al., 2005). NdhH-NdhK, NdhN, and NdhO were copurified with PSI from *Synechocystis* 6803 cells by Ni^{2+} affinity chromatography (Kubota et al., 2010). Zhao et al. (2014) showed that NdhO destabilized the NDH-1M and repressed the NDH-1 activity. In higher plants, absence of NdhN or NdhO caused the complete impairment of chloroplast NDH activity (Rumeau et al., 2005; Peng et al., 2012). However, because null alleles of *ndhN*, *ndhH*, or *NdhJ* have never been fully segregated in *Synechocystis* 6803, the localization and the function of these cyanobacterial subunits are still unknown. Here, by using an indirect route, we successfully constructed the fully segregated *ndhN*,

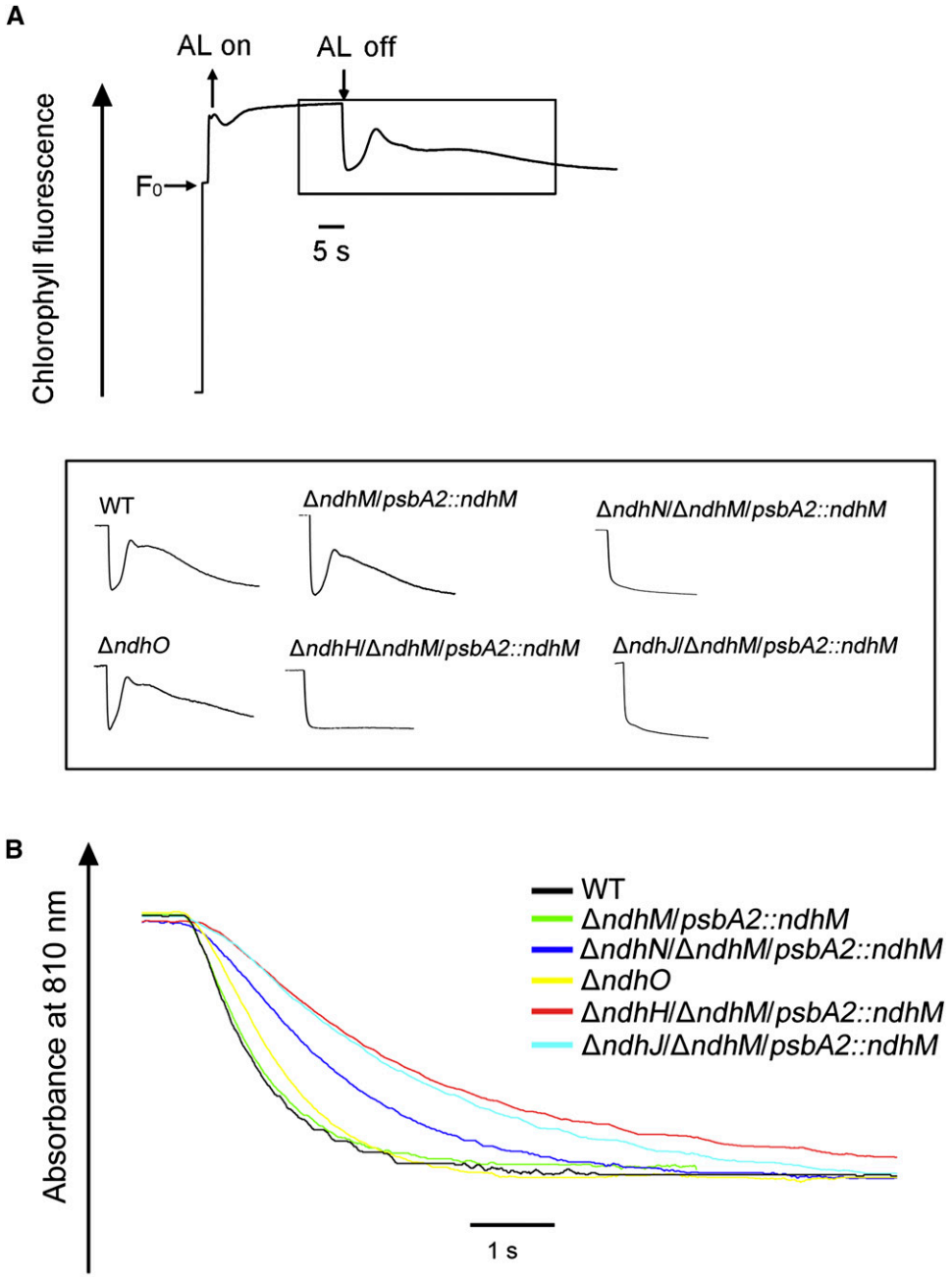

Figure 2. The effects on NDH-1 activity of the different NDH-1 mutants. A, Monitoring of the NDH-1 activity using chlorophyll fluorescence analysis. The upper curve shows a typical trace chlorophyll fluorescence in *Synechocystis* 6803. Cells were exposed to the AL (60 μmol photons m^{-2} s^{-1}) for 60 s. After it was switched off, the transient increase in chlorophyll fluorescence level was ascribed to NDH-1 activity. The inset shows the magnified traces from the box area. B, Kinetics of $P700^+$ rereduction in darkness after turning off far-red light in the presence of 10 μM DCMU. The chlorophyll *a* concentration was adjusted to 30 μg mL^{-1}, and curves are normalized to the maximal signal.

ndhH, and *NdhJ* null mutants. We demonstrate that absence of NdhN, NdhH, or NdhJ seriously impaired the hydrophilic subcomplexes of the NDH-1 complexes, resulting in the loss of the ability of CET and CO_2 uptake. Neither the NdhN nor NdhO deleted mutants affect the stability of the NDH-1 subcomplex assembly intermediates consisting of NdhK, NdhM, NdhH, and NdhJ in the cytoplasm. Based on these results, we proposed a new model of the NDH-1 complexes.

RESULTS

Deletion of *ndhN*, *ndhH*, and *ndhJ* Impairs NDH-1 Activity

To investigate the function of *ndhN*, *ndhO*, *ndhH*, and *ndhJ* genes in NDH-1 complexes, we constructed the mutants defective in these *ndh* genes. Genetic manipulations to generate the *ndhN*, *ndhH*, *ndhJ*, and *ndhO* null mutants are described in "Materials and Methods." The *ndhO* coding region was replaced with the gentamicin resistance (Gm^R) cassette. PCR analysis of the *ndhO*

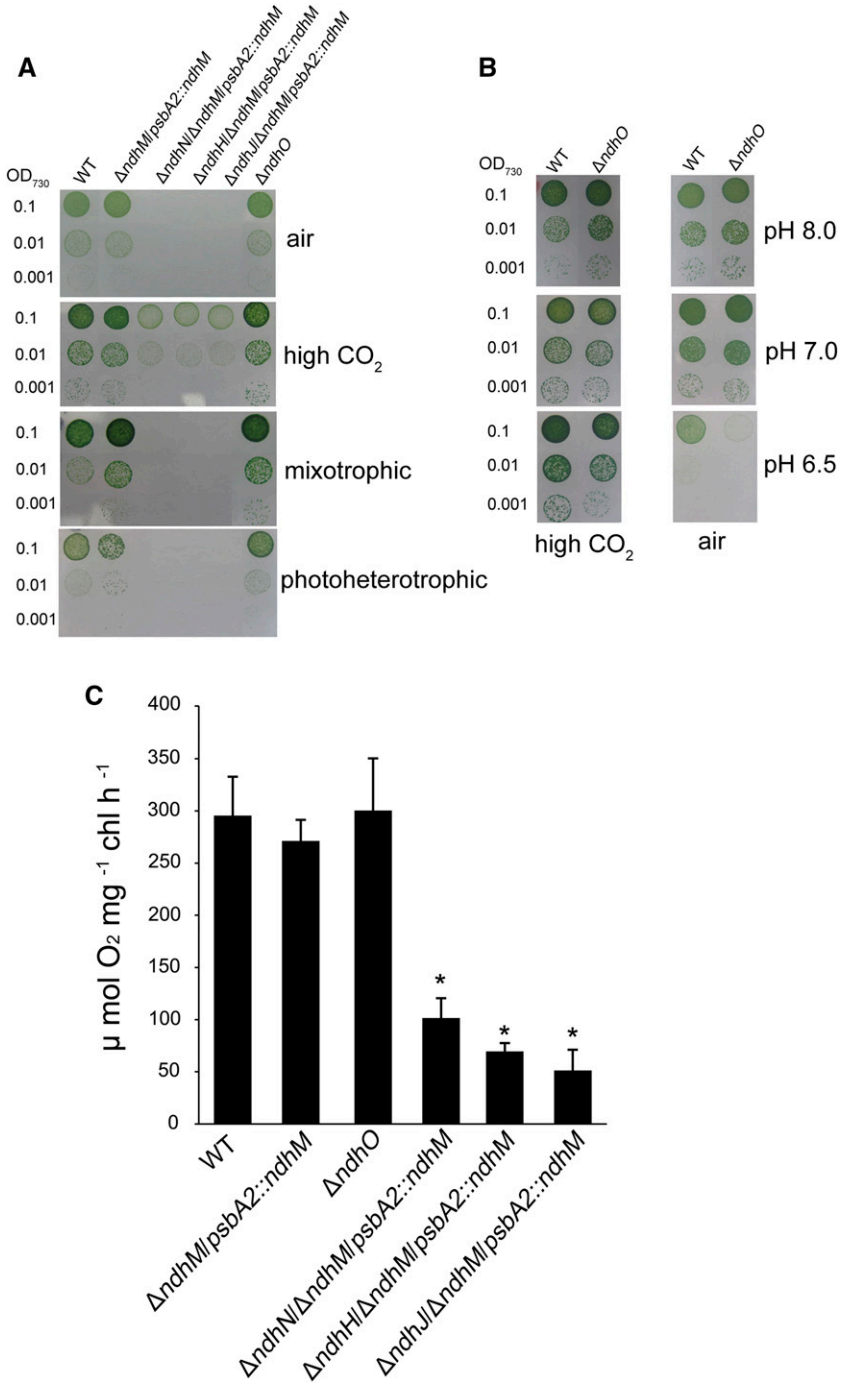

Figure 3. Growth and the oxygen evolution rates of the wild type and different NDH-1 mutant strains. A and B, Growth of wild-type, *ndhN*, *ndhH*, *ndhJ*, and *ndhO* deletion mutants. The concentration of the cells was adjusted to OD_{730} = 0.1, 0.01, and 0.001. Three microliters of the cell suspensions was placed on the agar plate with different carbon sources, and 3 μL of wild-type and Δ*ndhO* strains was spotted on the agar plates buffered at pH 8.0, 7.0, and 6.5. The cultures were grown for 7 d at 40 μmol photons m^{-2} s^{-1}. High CO_2, 2% CO_2 (v/v) in air; mixotrophic, BG-11 medium + 5 mM Glc; photoheterotrophic, BG-11 medium + 5 mM Glc + 10 μM DCMU. C, The rates of O_2 evolution of wild-type, *ndhN*, *ndhH*, *ndhJ*, and *ndhO*-deletion mutants using a light intensity of 400 μmol photons m^{-2} s^{-1} at 30°C. Values are means ± SE of three replicates. Asterisks indicate a significant difference from the wild type under the same growth conditions (Student's *t* test, $P < 0.05$).

locus confirmed the complete segregation of the *ndhO* allele (Fig. 1, B and D). Immunoblotting analysis using the antibody specifically prepared against NdhO demonstrated the absence of the gene product in the mutant (Fig. 4A). For construction of the *ndhN*, *ndhH*, and *ndhJ* null mutants, we used the Δ*ndhM* mutant strain in which the *ndhM* gene had been deleted and the hydrophilic subunits of NDH-1 complex could not be accumulated in the thylakoid membrane (He et al., 2016). The *ndhN*, *ndhH*, and *ndhJ* genes were inactivated in the Δ*ndhM* background. After several attempts, the fully segregated double mutant strains were obtained. Subsequently, the double mutant strains were respectively rescued at *psbA2* locus by transformation with a plasmid containing the fragment encoding for NdhM to produce the Δ*ndhN*/Δ*ndhM*/*psbA2*::*ndhM*, Δ*ndhH*/Δ*ndhM*/*psbA2*::*ndhM*, and Δ*ndhJ*/Δ*ndhM*/*psbA2*::*ndhM* mutant strains (Fig. 1A; Supplemental Fig. S1). To rule out the effect of *ndhM*, the control strain (Δ*ndhM*/*psbA2*::*ndhM*) was generated. Immunoblotting analysis using the antibodies against NdhN, NdhH, and NdhJ demonstrated the absence of the gene products in these mutant strains (Fig. 4A).

Next, we compared the NDH-1 CET activity among the *ndhN*, *ndhO*, *ndhH*, and *NdhJ* null mutants. We monitored the transient increase in chlorophyll a fluorescence after illumination with actinic light (AL), which is attributed to the NDH-dependent nonphotochemical reduction of the plastoquinone pool in the dark (Mi et al., 1995; Deng et al., 2003). In the absence of NdhN, NdhH, or NdhJ, the transient increase of chlorophyll fluorescence was completely arrested, whereas the NDH-1 CET activity was not affected in control strain (Δ*ndhM*/*psbA2*::*ndhM*; Fig. 2A). A previous study showed that the NDH-1 CET activity was higher in the NdhO deleted mutant (Zhao et al., 2014). In contrast, our measurements showed that the transient increase of chlorophyll fluorescence was slightly smaller in the Δ*ndhO* mutant compared with that in the wild type (Fig. 2A). A similar result was obtained by measuring the rereduction of $P700^+$ in darkness. P700 was oxidized by far-red light (>720 nm) for 40 s and then the subsequent rereduction of $P700^+$ in the dark was monitored. The operation of NDH-1 complexes transfers electrons from the reduced plastoquinone pool and accelerates the rereduction of $P700^+$ (Mi et al., 1995). The rereduction rate of $P700^+$ was decreased markedly in *ndhH* or *ndhJ* null mutants, partly in the *ndhN* null mutant strain, while only slightly in Δ*ndhO*, compared with that in the wild-type strain. No difference was observed between the Δ*ndhM*/*psbA2*::*ndhM* strain and the wild type (Fig. 2B). These results demonstrated that the three subunits (NdhN, NdhH, and NdhJ) are essential for the NDH-1 CET activity; however, the deletion of *ndhO* only slightly affected the NDH-1 CET activity.

Deletion of *ndhN*, *ndhH*, and *ndhJ* Results in the Growth Suppression Phenotype in Air or under Photoheterotrophic or Mixotrophic Conditions

In addition to CET around PSI, NDH-1 complexes are also involved in CO_2 uptake and respiration activities (Zhang et al., 2004). To examine the CO_2 uptake and respiration activities, wild-type, Δ*ndhM*/*psbA2*::*ndhM*, Δ*ndhN*/Δ*ndhM*/*psbA2*::*ndhM*, Δ*ndhH*/Δ*ndhM*/*psbA2*::*ndhM*, Δ*ndhJ*/Δ*ndhM*/*psbA2*::*ndhM*, and Δ*ndhO* strains were grown on BG-11 plates in the presence of 2% CO_2 in air or ambient air as well as under photoheterotrophic and mixotrophic conditions. The growth rates of *ndhN*, *ndhH*, and *ndhJ* deleted mutants were a bit slower than that of the wild type under autotrophic growth condition supplied

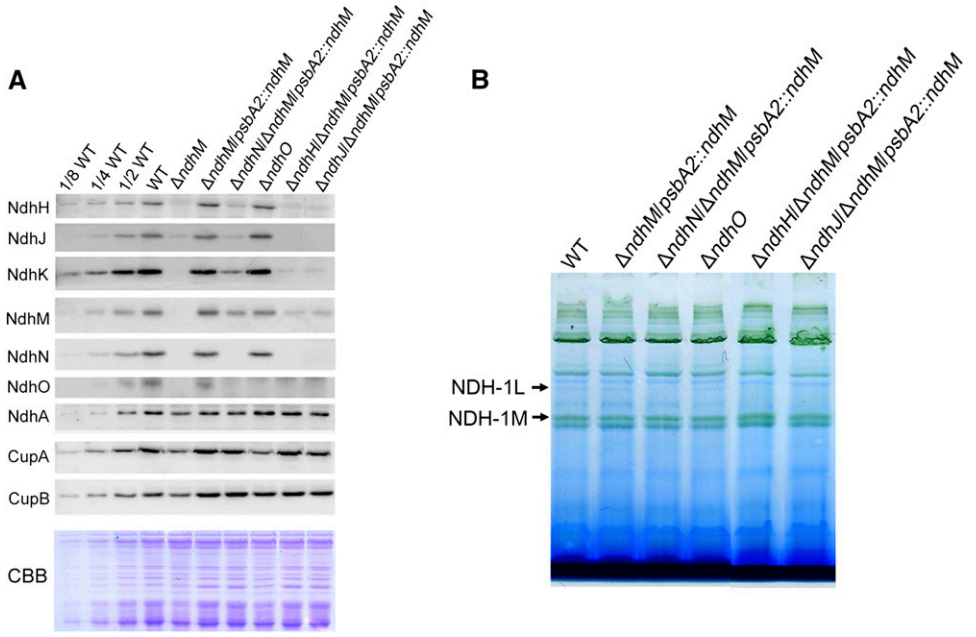

Figure 4. Analysis of the NDH-1 complex in different NDH-1 mutant backgrounds. A, Immunoblot analysis of Ndh subunits in thylakoid membranes of wild-type, *ndhM*, *ndhN*, *ndhO*, *ndhH*, and *ndhJ* deletion mutants. Each lane was loaded with thylakoid membrane proteins corresponding to 2 μg chlorophyll *a*, and the series of dilution is indicated. In the lower panel, a replicated gel stained with Coomassie Brilliant Blue (CBB) was used as a loading control. B, BN-PAGE analysis of thylakoid protein complexes isolated from wild-type, *ndhN*, *ndhO*, *ndhH*, and *ndhJ* deletion mutants. Each lane was loaded with thylakoid membrane proteins corresponding to 3 μg chlorophyll *a*.

with 2% CO_2, while they grew very poorly under air condition or photoheterotrophic or mixotrophic conditions (Fig. 3A).

The wild type and the control stain (Δ*ndhM*/*psbA2*::*ndhM*) behaved similarly under all growth conditions (Fig. 3A). No significant differences were observed between the Δ*ndhO* mutant and the wild-type cells under autotrophic (pH 8.0 or 7.0) or photoheterotrophic conditions (Fig. 3, A and B). The Δ*ndhO* mutant grew as fast as the wild type under the presence of 2% CO_2 at pH 6.5 (the concentration HCO_3^- becomes minor and CO_2 is predominant); nevertheless, the growth was slower than the wild type under air condition at pH 6.5 (both the concentrations of HCO_3^- and CO_2 are limited; Fig. 3B). Moreover, the *ndhO* mutant complemented with NdhO rescued a wild-type phenotype in air at pH 6.5 (Supplemental Fig. S3), confirming the slow growth phenotype caused by deletion of NdhO under the inorganic carbon limitation condition. Based on these results, we show that deletion of *ndhO* partially impaired the CO_2 uptake activity. We further compared the capacity of photosynthesis among the wild type and the mutants as reflected by O_2 evolution. Figure 3C shows that the rates of oxygen evolution were significantly reduced to about 30% in *ndhN* and about 20% in *ndhH or ndhJ* deleted mutants of that in wild-type strain, while the rate of *ndhO* deleted mutant was similar with that in the wild type. The above results suggest that in addition to NDH-1 CET, NdhN, NdhH, and NdhJ are essential for respiration and CO_2 uptake and NdhO functions under the inorganic carbon limitation condition.

Disassembly of NDH-L, NDH-1MS, and NDH-1MS′ in *ndhN*, *ndhH*, and *ndhJ* Null Mutants

To investigate how NDH-1 activity is affected in the absence of NdhN, NdhH, NdhJ, or NdhO, we compared the accumulation of the NDH-1 complexes in the thylakoid membranes of the wild type and various NDH-1 mutant strains, including *ndhM*, *ndhN*, *ndhH*, *ndhJ*, and *ndhO* null mutants, by immunoblotting analysis using antibodies against NdhH, NdhJ, NdhK, NdhM, NdhN, NdhO, CupA, and CupB. As shown in Figure 4A, similar to the Δ*ndhM* mutant, inactivation of *ndhH* or *ndhJ* almost completely abolished accumulation of the subunits of the hydrophilic domain of the NDH-1 complex, while the accumulation of the NdhA from the hydrophobic domain embedded in the membrane was not affected. The levels of NdhH, NdhJ, NdhK, NdhM, and NdhO were reduced to less than one-fourth of the wild type in the absence of NdhN, while the accumulation of the CupA and CupB was slightly affected in the mutant. In contrast, the accumulation of other Ndh subunits was barely affected in the absence of NdhO.

Furthermore, to reveal how the NDH-1 complexes are affected in different NDH-1 mutant strains, we separated the protein complexes from thylakoid membranes in the mutants by a 5 to 13% gradient Blue native-PAGE (BN-PAGE; Fig. 4B) and observed that the band corresponding to the NDH-1L complex disappeared in the *ndhN*, *ndhH*, and *ndhJ* null mutants, but not in the *ndhO* null mutant. Since the NDH-1L band was very weak in the BN gel, we further confirmed the results by two-dimensional SDS-PAGE and immunoblotting with antibodies against several Ndh subunits

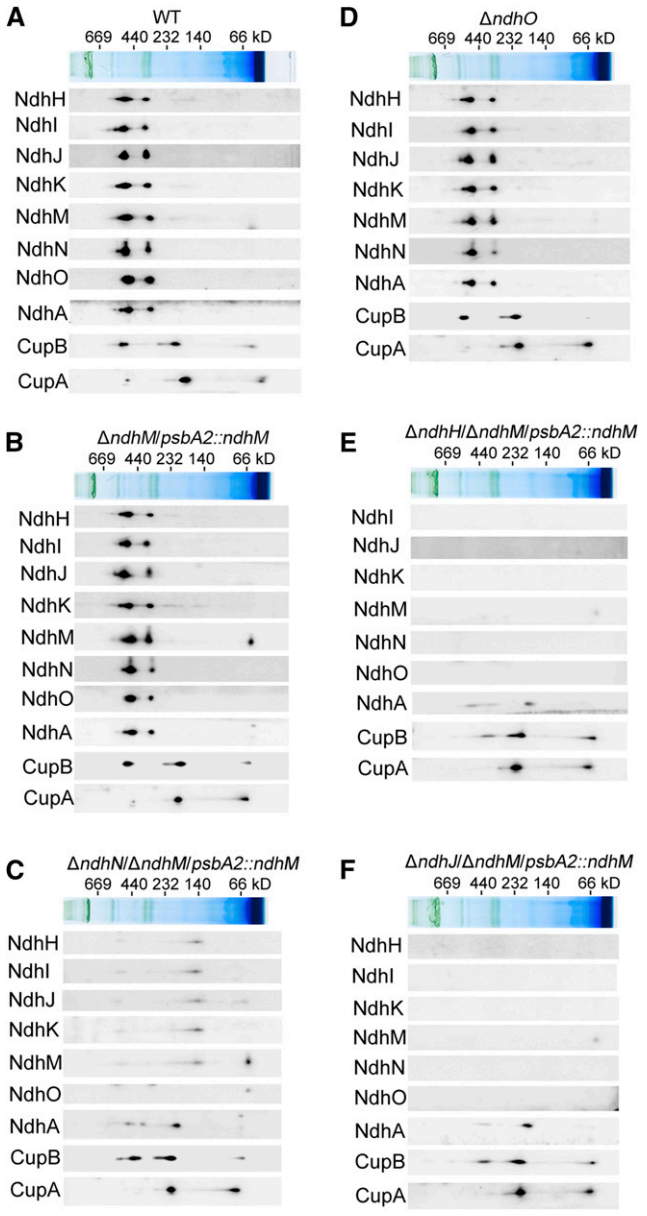

Figure 5. Accumulation of Ndh subunits and their assembly into the NDH-1L and NDH-1M complexes in the thylakoid membranes of different NDH-1 mutant backgrounds. A-F, Thylakoid membrane proteins from the wild type and indicated mutant strains were separated by BN-PAGE and further subjected to 2D/SDS-PAGE. The proteins were immunodetected with the indicated antibodies against the Ndh subunits. The positions of molecular mass markers in the BN gel are indicated.

(Fig. 5). Indeed, both the NDH-1L and NDH-1M complexes were disassembled in the *ndhN* deleted mutant. The amount of the hydrophilic subunits, including NdhH, NdhI, NdhJ, NdhK, and NdhM, was evidently decreased and was present in a subcomplex with a molecular mass of ~140 kD. The hydrophobic subunit, NdhA, was present in a subcomplex with a approximate molecular mass of 200 kD (Fig. 5C). In contrast, the accumulation of the NDH-1L and NDH-1M complexes in the Δ*ndhO* and Δ*ndhM*/*psbA2*::*ndhM* was not influenced (Fig. 5, B and D). Moreover, we also checked the low CO_2-induced NDH-1MS and the constitutively expressed NDH-1MS′ complexes, which are essential for CO_2 uptake activity. As shown in Figure 5A, NDH-1MS complex, NDH-1S complex, and free protein could be detected in the wild type using the antibody against CupA. However, in the absence of NdhN, NdhH, or NdhJ, only the NDH-1S complex and the free CupA could be detected, while the NDH-1MS complex was absent in the thylakoid membranes (Fig. 5, C, E, and F). Similarly, the NDH-1MS′ complex, NDH-1S′ complex, and free protein could also be detected in the wild type and control strains using the antibody against CupB. In the *ndhN*, *ndhH*, and *ndhJ* deleted mutants, the accumulation of the NDH-1S′ complex and the free CupB was not affected; however, the NDH-1MS′ complex with a molecular mass of ~550 kD was degraded to a subcomplex with ~400 kD, lacking the hydrophilic Ndh subunits (Fig. 5, C, E, and F). Nevertheless, the accumulation of the NDH-1MS and the NDH-1MS′ complex was not impaired in the Δ*ndhO* mutant (Fig. 5D). Taken together, our results demonstrate that in the absence of NdhN, the amount of the hydrophilic subunits was significantly decreased and the remaining entire NDH-1 complexes were degraded to the hydrophilic subcomplex and hydrophobic subcomplex, while the absence of the NdhH or NdhJ caused the disassembly of the hydrophilic subcomplex of NDH-1 complexes; by contrast, the absence of NdhO appeared not to impair the stability of the NDH-1 complexes.

The Interaction of NdhN or NdhO with Other Ndh Subunits

To determine the interaction of NdhN or NdhO with other hydrophilic Ndh subunits, we generated

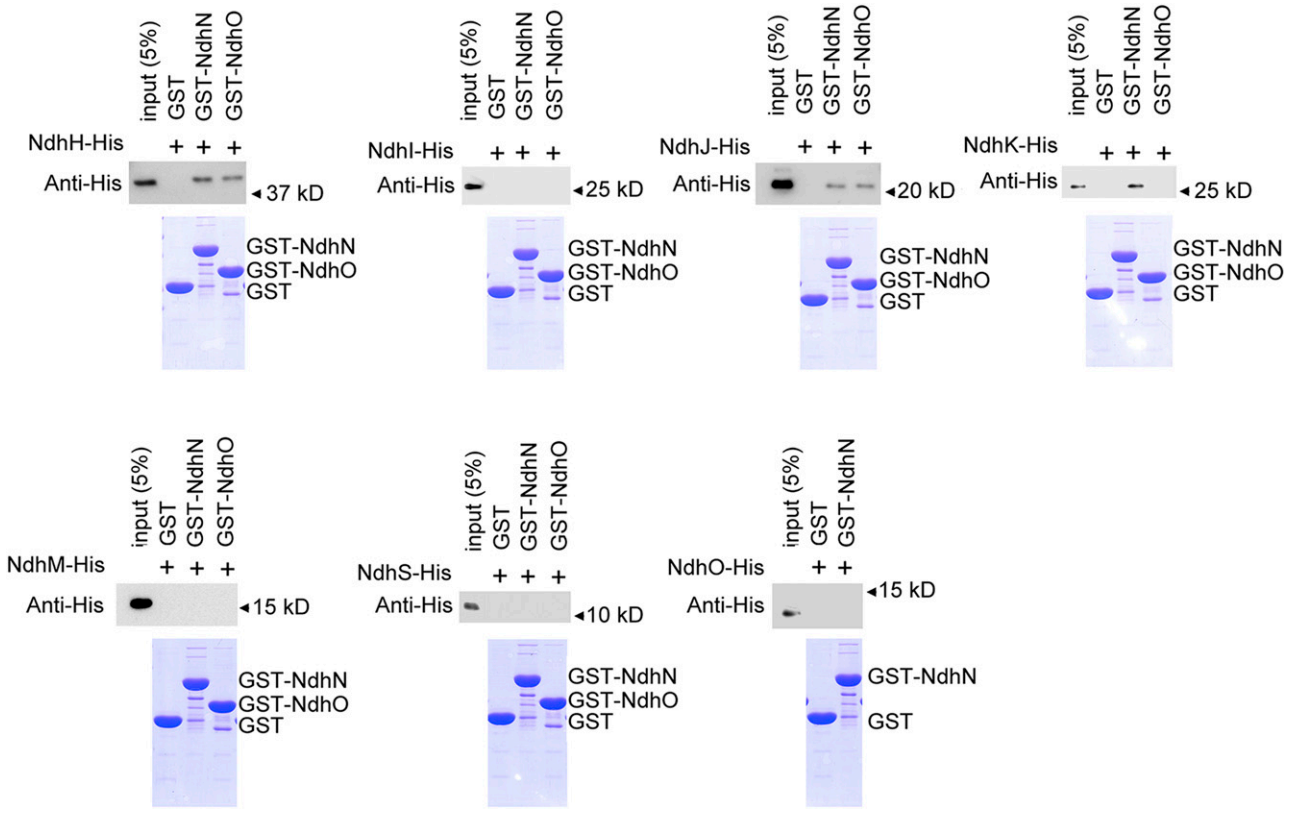

Figure 6. Pull-down analysis of NdhN and NdhO with other Ndh subunits. Recombinant His-tagged NdhH, NdhI, NdhJ, NdhK, NdhM, and NdhS were incubated with recombinant GST, NdhN fused to GST, and NdhO fused to GST, respectively. The recombinant His-tagged NdhO was also incubated with recombinant GST and NdhN fused to GST. Proteins were bound to the GST affinity resin and then eluted with Laemmli buffer. Eluates were analyzed by SDS-PAGE and Coomassie blue staining, and the Ndh subunits were detected by immunoblot with anti-His antibody.

recombinant NdhN and NdhO fused with GST. The recombinant NdhH-$(His)_6$, NdhI-$(His)_6$, NdhJ-$(His)_6$, NdhK-$(His)_6$, NdhM-$(His)_6$, NdhS-$(His)_6$, and NdhO-$(His)_6$ fusion proteins were then generated and tested for the interaction with GST-NdhN or GST-NdhO. GST-NdhN or GST-NdhO was bound to a GST affinity column and used as bait. Recombinant GST was used as negative control for unspecific binding. Proteins were eluted using Laemmli buffer and analyzed by immunoblotting (Fig. 6). These in vitro pull-down experiments show that NdhN interacts with NdhH, NdhJ, and NdhK, but not with NdhI, NdhM, NdhO, or NdhS subunits. As shown in Figure 6, NdhO only interacts with NdhH and NdhJ.

Analyses of NDH-1 Assembly Intermediates under Various Mutant Backgrounds

To know whether the defect of the four subunits (NdhN, NdhH, NdhJ, and NdhO) affects the assembly of NDH-1 complex, we investigated the components of the NDH-1 assembly intermediates by Clear native-PAGE (CN-PAGE) and subsequent immunoblot analyses for the cytoplasmic fraction under various mutant backgrounds. Our previous results demonstrated that the NDH-1 assembly intermediates, including NdhH, NdhK, and NdhM, were seriously affected in the Δ*ndhM* or Δ*ndhK* mutant (He et al., 2016). Here, we generated a new antibody against NdhJ of *Synechocystis* 6803 and showed that in the wild type, NdhH, NdhJ,

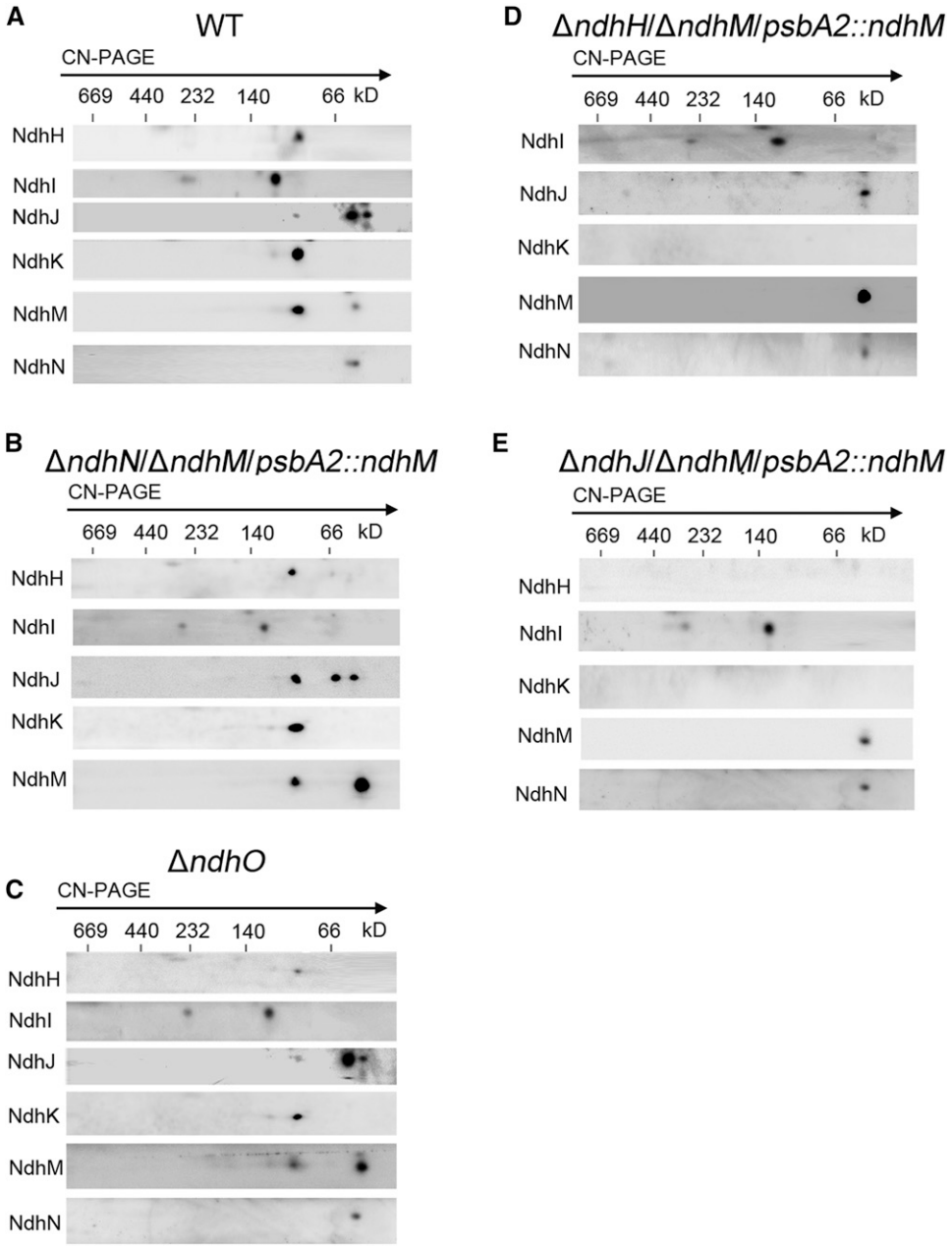

Figure 7. Analysis of the cytoplasmic intermediate complexes isolated from the wild type and various NDH-1 mutant strains. A to E, Cytoplasmic protein complexes isolated from the wild type and the various mutants were separated by CN-PAGE and further subjected to 2D/SDS-PAGE. The proteins were immunodetected with antibodies against Ndh subunits (NdhH, NdhI, NdhJ, NdhK, NdhM, and NdhN). The positions of molecular mass markers are indicated.

NdhK, and NdhM subunits were present in a subcomplex with an apparent molecular mass of ~100 kD, and NdhJ was also detected in a subcomplex of ~60 kD as well as free protein, while NdhI was present in two subcomplexes with approximate molecular masses of 300 and 130 kD (Fig. 7A). However, the NdhN subunit was only detected as free protein, and in the absence of NdhN, the NDH-1 assembly intermediates, including NdhH, NdhJ, NdhK, and NdhM, or assembly intermediates containing NdhI were not affected (Fig. 7, A and B). Similarly, in the Δ*ndhO* mutant, the NDH-1 assembly intermediates are formed efficiently in the cytoplasm (Fig. 7C). These results suggested that NdhN or NdhO appeared to be integrated to the NDH-1 complex in later steps of assembly (Fig. 8).

The mutant defective in NdhH failed to accumulate the 100-kD NDH-1 assembly intermediate consisting of NdhJ, NdhK, and NdhM. Only free NdhM, NdhJ, and NdhN could be detected in the mutant (Fig. 7D). Similar to the NdhH deleted mutant, the 100-kD assembly intermediate was also undetectable in the NdhJ deleted mutant (Fig. 7E). Nevertheless, the 300- and 130-kD assembly intermediates consisting of NdhI and other unknown proteins were not affected in all the mutant backgrounds (Fig. 7, B–E). These results indicated that NdhH and NdhJ are necessary for the stability of the NDH-1 assembly intermediate of 100 kD, and the assembly process of NdhI was independent of other Ndh subunits (Fig. 8).

DISCUSSION

NdhN, NdhH, and NdhJ Are Required for Stability of NDH-1 Complexes Involved in CET around PSI, Respiratory Electron Transport, and CO_2 Uptake

Cyanobacterial NDH-1 complexes have multiple functions because of the diversity of the complexes based on their different subunits composition. Although great progress has been made in revealing the functions of novel subunits of NDH-1, the localization and the function of several subunits still need to be elucidated (Ogawa and Mi, 2007; Battchikova et al., 2011a; Ma and Ogawa, 2015). The NdhN and NdhO subunits exclusively exist in oxygenic photosynthetic organisms (Prommeenate et al., 2004; Rumeau et al., 2005). In higher plants, the chloroplast NDH complex interacts with PSI complex to form a supercomplex. The chloroplast NDH complex is divided into five subcomplexes, consisting of subcomplex A, membrane subcomplex, subcomplex B, lumenal subcomplex, and electron donor binding subcomplex (Ifuku et al., 2011). The hydrophilic subunits corresponding to NdhH-K and NdhM-O, including NdhL, are grouped into subcomplex A. The membrane-spanning subunits corresponding to NdhA-G form the membrane subcomplex. Both the subcomplex A and membrane subcomplex are conserved in cyanobacteria (Peng et al., 2009). Knockout of *ndhN* or *ndhO* results in complete loss of NDH activity and entire collapse of subcomplex A of chloroplast NDH complex (Rumeau et al., 2005; Peng et al., 2009, 2012).

Because the fully segregated *ndhN* null mutant could not be directly obtained in *Synechocystis* 6803, the function of cyanobacterial NdhN remains elusive. In this work, we deleted the *ndhN* gene in the Δ*ndhM* strain and then we rescued the *ndhM* gene at the *psbA2* locus. By investigation of the mutant, we found that deletion of NdhN caused the significant decrease of hydrophilic subunits levels (Fig. 4A), resulting in disassembly of NDH-1MS, NDH-1MS′, as well as NDH-1L (Fig. 5C), thus causing the inactivation of NDH-1 (Fig. 1). The severe growth suppression phenotype of NdhN, NdhH, or NdhJ deleted mutants under air condition or in the presence of Glc (Fig. 3A) suggests that NdhN, NdhH, and NdhJ are essential for NDH-1 CET, CO_2 uptake, and respiration.

In contrast, the NDH-1 activity was only slightly impaired in the Δ*ndhO* mutant, although it was conflict with the observation in the previous study (Zhao et al., 2014). The deletion of NdhO indeed didn't affect the growth at pH 8.0 at high CO_2 condition (2% CO_2 in air), but the growth was suppressed under atmospheric levels of CO_2, especially at pH 6.5 (Fig. 3B), where

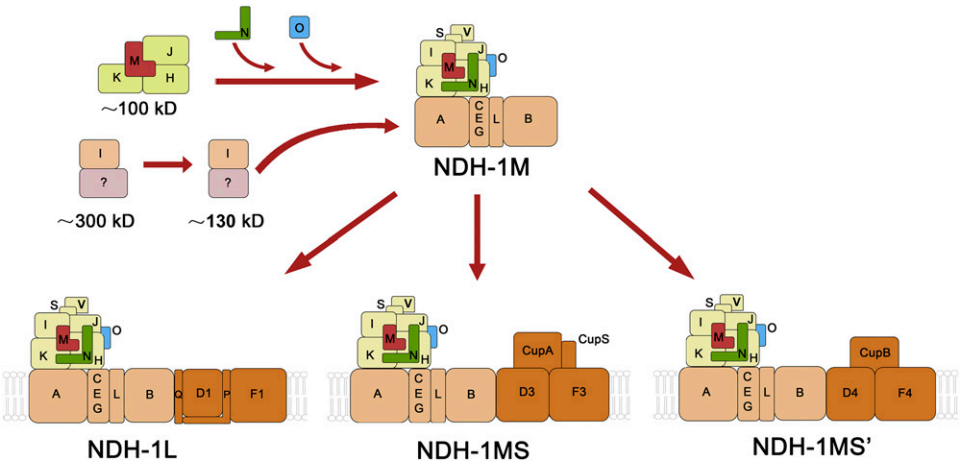

Figure 8. A schematic model of cyanobacterial NDH-1 complex assembly. NdhH, NdhJ, NdhK, and NdhM are first assembled to form a 100-kD complex. Meanwhile, NdhI, as well as unknown factors, are assembled to form the 130- kD complex and the 300-kD complex. Subsequently, NdhN, NdhO, and NdhI are assembled to form the NDH-1M complex. The basic complex NDH-1M is combined with specific domains to assemble the functional complexes NDH-1L, NDH-1MS, and NDH-1MS′.

HCO_3^- was minor (Ohkawa et al., 2000). The result suggests that NdhO functions in CO_2 uptake under the condition of inorganic carbon limitation. On the other hand, as shown in Figure 6, NdhO interacts with NdhH and NdhJ. However, Zhao et al. (2014) showed that NdhO interacts with NdhI and NdhK, but not with other Ndh subunits, using the yeast two-hybrid system. Further experiments including 3D structure analysis are necessary to resolve the controversy.

Localization of NdhN, NdhH, and NdhJ in NDH-1 Complexes

A previous study demonstrated that NdhL-NdhO subunits are grouped together in the central part of membrane domain of cyanobacterial NDH-1 complexes (Birungi et al., 2010), while it was suggested that NdhL, NdhM, NdhN, and NdhO are subunits of subcomplex A of chloroplast NDH in Arabidopsis (Peng et al., 2009). In this work, we proposed that cyanobacterial NdhN or NdhO, together with NdhM, are localized in the hydrophilic arm, corresponding to the subcomplex A in Arabidopsis.

In Arabidopsis, various NDH assembly intermediates exist in chloroplast stroma. Three assembly intermediates with approximate apparent molecular masses of 800, 500, and 300 kD contain NdhH in the stroma. The folding of NdhH requires the Cpn60 complex containing Cpn60β4 (Peng et al., 2011). The native NdhH, NdhO, CRR41, and other unknown proteins form the 500-kD assembly intermediate, which provides a scaffold for the assembly of NdhI, NdhJ, NdhK, and NdhM to form the 400-kD assembly intermediate (Peng et al., 2012). However, in the cytoplasm of *Synechocystis* 6803, NdhH, NdhJ, NdhK, and NdhM form the 100-kD assembly intermediate (Fig. 7). The molecular mass for the sum of four subunits is 107.6 kD, indicating that the 100-kD assembly intermediate does not contain other assembly factors. Interestingly, by constructing a *Synechocystis* 6803 strain with a His_6 tag in the C terminus of NdhJ, Prommeenate et al. (2004) isolated three NdhJ-containing complexes with approximate apparent molecular masses of 460, 330, and 110 kD, implying the fragility of the NDH-1L. Further mass spectrometry analysis demonstrated that the 110-kD subcomplex was composed of NdhH, NdhJ, NdhK, and NdhM (Prommeenate et al., 2004). Our result showed the direct evidence that deletion any of the four subunits causes the disassembly of the 100 kD assembly intermediate (Fig. 7). Our recent studies demonstrated that the formation of 100 kD assembly intermediate was not impaired in the Δ*ndhI* mutant (He et al., 2016). For some unknown reason, Peng et al. (2012) could not detect NdhI in the 2D CN/SDS-PAGE in chloroplast stroma. We showed that NdhI and other unknown proteins form the 300- and 130-kD assembly intermediates in the cytoplasm of *Synechocystis* 6803, which were not affected in all the mutant backgrounds (Fig. 7), indicating that the formation of these assembly intermediates appeared to be dependent on other assembly factors (Fig. 8), probably Slr1097, homolog of CRR6 in Arabidopsis, involved in the maturation of NdhI (Dai et al., 2013).

In addition, we showed that the cyanobacterial NDH-1 assembly intermediates were not affected in *ndhO* mutant, while in Arabidopsis, it was shown that NdhO together with NdhH are essential for the formation of the 500- and 400-kD assembly intermediates (Peng et al., 2012). The NdhN was present as free protein, and we could not detect NdhO in the cytoplasm of the wild type, suggesting that NdhN and NdhO are incorporated to the NDH-1 complexes after the formation of the NDH-1 assembly intermediates (Fig. 8). Consistent with chloroplast NDH complex, the cyanobacterial NDH-1 complex assembly intermediates were not affected in the *ndhN* null mutant.

Recent years have seen steady progress toward the atomic resolution structures of intact complex I from *Thermus thermophilus* (Baradaran et al., 2013), *Bos taurus* (Vinothkumar et al., 2014), and *Yarrowia lipotytica* (Zickermann et al., 2015). The cyanobacterial NDH-1 complex is homologous to the respiratory complex I except the OPS Ndh subunits. Cyanobacterial NdhH, NdhI, NdhJ, and NdhK are related to Nqo4, Nqo9, Nqo5, and Nqo6 in *T. thermophilus*, or mitochondrial 49-kD, TYKY, 30-kD, and PSST subunits, respectively, which are highly conserved from bacteria to humans. Nqo1 to Nqo3 form the dehydrogenase domain whose homologs do not exist in cyanobacteria, and the subunits Nqo4 to Nqo6 and Nqo9 connect it to the membrane arm. Nqo9 coordinates the Fe-S clusters N6a and N6b, while Nqo6 coordinates cluster N2 at the interface of Nqo4 (Sazanov and Hinchliffe, 2006). The 49-kD subunit, corresponding to NdhH, comprises a prominent four-helix bundle inclined toward the membrane surface, suggesting the binding of the peripheral arm of complex I to the membrane domain (Zickermann et al., 2015). Nqo5, homolog of NdhJ in *Synechocystis* 6803, wraps around Nqo4 on one side and interacts also with Nqo9. It was suggested that the role of Nqo5 is to stabilize the complex I (Sazanov and Hinchliffe, 2006). So far, the atomic resolution structure of cyanobacterial NDH-1 complex was not available. In our study, we found that NdhN interacts with NdhH, NdhJ, and NdhK, while NdhO interacts with NdhH and NdhJ (Fig. 6). Therefore, structurally, cyanobacterial NdhH-K are conserved with bacterial complex I and the position of NdhM-O is also conserved with chloroplast NDH. We suggest that NdhN is localized adjacent to the hydrophilic subunits and NdhO is localized between NdhH and NdhJ, as shown in the new NDH-1 complexes model (Fig. 8).

In conclusion, this study demonstrates that the cyanobacterial NdhN, NdhH, and NdhJ subunits, localized in the hydrophilic arm of the NDH-1 complexes, are required for stability of the NDH-1 complexes involved in CET around PSI, respiratory electron transport, and CO_2 uptake. In addition, NdhO functions in

the efficient NDH-1 activity under the condition of inorganic carbon limitation.

MATERIALS AND METHODS

Culture Conditions

The Glc-tolerant strain of the wild-type *Synechocystis* 6803 and mutants, Δ*ndhM* (He et al., 2016), Δ*ndhM*/*psbA2*::*ndhM*, Δ*ndhN*/Δ*ndhM*/*psbA2*::*ndhM*, Δ*ndhH*/Δ*ndhM*/*psbA2*::*ndhM*, Δ*ndhJ*/Δ*ndhM*/*psbA2*::*ndhM*, and Δ*ndhO* were cultured at 30°C in BG-11 medium (Allen, 1968), buffered with Tris-HCl (5 mM, pH 8.0), and bubbled with 5% (v/v) CO_2 in air. The solid medium used was BG-11 supplemented with 1.5% agar. Continuous illumination was provided by fluorescence lamps at 60 μmol photons m^{-2} s^{-1}.

Construction of Mutant Strains

The upstream and downstream regions of *ssl1690* (*ndhO*) were amplified by PCR creating appropriate restriction sites. A DNA fragment encoding a gentamicin resistance (Gm^R) cassette was also amplified by PCR, creating *Kpn*I and *Bam*HI sites using specific oligonucleotide primers (Supplemental Table S1). These three products were ligated into the MCS of pUC19 (Fig. 1B), which was used to transform the wild-type cells of *Synechocystis* 6803 as described by Williams and Szalay (1983). The transformants were spread on agar plates containing BG-11 medium and gentamicin (5 μg mL^{-1}) buffered at pH 8.0, the plates were incubated in 2% (v/v) CO_2 in air, and continuous illumination was provided by fluorescence lamps at 60 μmol photons m^{-2} s^{-1}. The mutated *ndhO* in the transformants was segregated to homogeneity as determined by PCR amplification and immunoblotting. The same strategy was used for constructing the Δ*ndhN*, Δ*ndhH*, and Δ*ndhJ* mutants; nevertheless, direct deletion of *ndhN*, *ndhH*, and *ndhJ* was never successful. Thus, a different strategy was used. First, we used the Δ*ndhM* strain we recently constructed. The *ndhN*, *ndhH*, and *ndhJ* genes in these strains were deleted by replacing parts of the genes with a DNA fragment encoding kanamycin resistance (Km^R) cassette, respectively. The generated Δ*ndhN*/Δ*ndhM*, Δ*ndhH*/Δ*ndhM*, and Δ*ndhJ*/Δ*ndhM* mutants were respectively rescued at *psbA2* locus by transformation with the pPSBA2 vector inserted with a chloramphenicol resistance (Cm^R) gene (Lagarde et al., 2000) containing the fragment encoding for NdhM to produce the Δ*ndhN*/Δ*ndhM*/*psbA2*::*ndhM*, Δ*ndhH*/Δ*ndhM*/*psbA2*::*ndhM*, and Δ*ndhJ*/Δ*ndhM*/*psbA2*::*ndhM* mutant strains. The Δ*ndhM* mutant was also transformed with this vector to generate the Δ*ndhM*/psbA2::*ndhM* strain (Fig. 1A; Supplemental Fig. S1). To complement the *ndhO* mutant, the *ndhO* mutant was also rescued at *psbA2* locus by transformation with the pPSBA2 vector containing the fragment encoding for NdhO to produce the Δ*ndhO*/*psbA2*::*ndhO* strain (Supplemental Fig. S2). The PCR primers used to amplify the flanking sequence regions are listed in Supplemental Table S1. Full segregation of all mutants was confirmed by PCR.

Measurement of Chlorophyll Fluorescence and Redox Kinetics of P700

The transient increase in chlorophyll fluorescence after AL had been turned off was monitored by means of using a PAM Chl fluorometer (Walz), emitter-detector-cuvette assembly (ED-101US), and unit 101ED as previously described (Mi et al., 1995; Deng et al., 2003). After dark acclimation for 30 min, samples were exposed to actinic red light (~630 nm, 60 μmol photons m^{-2} s^{-1}) for 60 s, and the kinetics of PSII chlorophyll fluorescence after switching off actinic illumination was recorded as a measure of NDH activity.

The redox kinetics of P700 was measured as previously described (Mi et al., 1995; Deng et al., 2003). The rereduction of $P700^+$ in darkness was measured using the PAM Chl fluorometer, ED-101US, and a unit ED-P700DW-II, by monitoring absorbance changes at 830 nm and using 875 nm as a reference. Cells were kept in the dark for 2 min, and 10 μM 3-(3,4-dichlorophenyl)-1,1dimethylurea (DCMU) was added to the cultures prior to measurement. P700 was oxidized by far-red light (>720 nm, 16 μmol photons m^{-2} s^{-1} from an LED lamp for 40 s), and the subsequent rereduction of $P700^+$ in the dark was monitored.

Oxygen Evolution Measurements

The rate of O_2 evolution was determined using a Clark type O_2 electrode at 30°C as described by Wu et al. (2011). The cells were harvested by centrifugation and resuspended in a fresh growth medium at a chlorophyll concentration of 10 μg/mL. The measurements were performed with actinic white light (400 μmol photons m^{-2} s^{-1}).

Isolation of Crude Thylakoid Membranes and Soluble Cell Fractions

Thylakoid membranes from *Synechocystis* 6803 were isolated as described by Gombos et al. (1994) with some modifications as follows. Cell cultures (1 liter) were harvested, resuspended in 5 mL disruption buffer (10 mM HEPES-NaOH, 5 mM sodium phosphate, pH 7.5, 10 mM $MgCl_2$, 10 mM NaCl, and 20% [v/v] glycerol), broken by shaking with glass beads (150–212 μm), and then centrifuged at 5000*g* for 5 min at 4°C to remove glass beads and unbroken cells. The crude thylakoid membranes were obtained by centrifugation of the supernatant at 20,000*g* for 30 min at 4°C. The soluble fractions were separated by further centrifugation at 100,000*g* for 30 min. The thylakoid membranes were suspended in solubilization buffer (20 mM BisTris-HCl, pH 7.0, 10 mM $MgCl_2$, and 20% [v/v] glycerol) at a final chlorophyll concentration of 1 mg mL^{-1}.

Electrophoresis and Immunoblotting

BN-PAGE of the thylakoids membranes from *Synechocystis* 6803 was performed as described previously (Kügler et al., 1997) with slight modifications as follows. Membranes were washed with 330 mM sorbitol and 50 mM BisTris-HCl, pH 7.0, and solubilized in 25 mM BisTris-HCl, pH 7.0, 10 mM $MgCl_2$, and 20% (v/v) glycerol at a chlorophyll a concentration of 0.5 mg mL^{-1}. After incubation on ice for 40 min with 2% *n*-dodecyl β-D-maltoside and centrifugation at 20,000*g* for another 15 min, the supernatants were supplemented with one-tenth volume of BN sample buffer (5% Serva Blue G, 100 mM BisTris-HCl, pH 7.0, 30% [w/v] Suc, 500 mM ε-amino-*n*-caproic acid, and 10 mM EDTA). Solubilized membranes were then applied to a 0.75-mm-thick 5 to 13% acrylamide gradient gel. Electrophoresis was performed at 4°C by increasing the voltage gradually from 50 to 200 V during the 5-h run. The lanes of the BN gel were cut out and incubated in Laemmli SDS sample buffer containing 5% β-mercaptoethanol for 30 min. SDS-PAGE of the membrane protein was performed on a 12% polyacrylamide gel as described previously (Laemmli, 1970).

CN-PAGE of the soluble cell fractions from *Synechocystis* 6803 was performed as described previously (Peng et al., 2012) with slight modifications. A total of 50 μg cytoplasmic proteins was mixed with one-quarter volume of sample buffer (40 mM BisTris-HCl, pH 7.0, 0.008% Ponceau S, 200 mM ε-amino-*n*-caproic acid, and 60% [v/v] glycerol). Cytoplasmic proteins were separated by 5 to 13% acrylamide gradient CN-PAGE in 0.75-mm-thick gels. Electrophoresis was performed at 4°C by increasing the voltage gradually from 50 to 200 V during the 4-h run. The lanes of the CN gel were cut out and incubated in Laemmli SDS sample buffer containing 5% β-mercaptoethanol for 30 min. SDS-PAGE of the proteins was performed on a 12% polyacrylamide gel.

For immunoblotting, the proteins in gel were electrotransferred to a polyvinylidene difluoride membrane (Immobilon-P; Millipore) and detected using protein-specific antibodies with the ECL assay kit (Thermo Scientific) according to the manufacturer's protocol. Antibodies against the NdhN, NdhO, and NdhJ proteins of *Synechocystis* 6803 were raised in our laboratory. Primer sequences used to amplify the *ndhN*, *ndhO*, and *ndhJ* genes are listed in Supplemental Table S1. The PCR products were ligated into vector pET28a (+) (Novagen). The plasmids were used to transform *Escherichia coli* strain BL21 (DE3) pLysS for expression. Polyclonal antibodies were raised in rabbits from purified recombinant proteins. The antibodies against NdhH, NdhI, NdhK, NdhA, CupA, and CupB were previously raised in our laboratory.

Expression and Purification of Fusion Proteins

For testing the direct interactions of NdhN and NdhO with other Ndh subunits, the fragments containing *ndhH*, *ndhI*, *ndhJ*, *ndhK*, *ndhM*, *ndhS*, and *ndhO* genes were amplified by PCR and cloned into pET28a(+) to form His-tagged fusion protein constructs. The fragments containing *ndhN* and *ndhO* were cloned into pGEX-4T-1 to form the GST-tagged fusion constructs. Primer sequences used are listed in Supplemental Table S1. These constructs were transformed into *E. coli* strain BL21 (DE3) pLysS and induced by 1 mM isopropyl-β-D-thiogalactoside for 16 h at 16°C. These fusion proteins were purified using a nickel column (GE Healthcare) and glutathione Sepharose 4B (GE Healthcare) column according to the manufacturer's instructions.

GST Pull-Down Assay

GST-NdhN, GST-NdhO, or GST and His-tagged fusion proteins were incubated with 20 μL glutathione Sepharose 4B rein for 2 h at 4°C in a buffer containing 20 mM Tris-HCl, pH 7.5, 100 mM NaCl, 0.1 mM EDTA, 0.2% (v/v) Triton, and 10% (v/v) glycerol. The protein-bound resin was washed five times with a buffer containing 20 mM Tris-HCl, pH 7.5, 300 mM NaCl, 0.1 mM EDTA, and 0.5% (v/v) Nonidet P-40. The washed proteins were directly eluted with Laemmli buffer at 95°C for 5 min. The input and eluates were analyzed by immunoblotting and Coomassie staining.

Accession Numbers

Sequence data from this article can be found in the GenBank/EMBL data libraries under accession numbers Sll1262 (BAA18145.1), Slr0261 (BAA17939.1), Slr1281 (BAA18285), and Ssl1690 (BAA10471.1).

Supplemental Data

The following supplemental materials are available.

Supplemental Figure S1. Construction and verification of the *ndhH*-deletion and *ndhJ*-deletion mutants.

Supplemental Figure S2. Construction and verification of the complemented *ndhO* strain.

Supplemental Figure S3. Growth of the wild type, *ndhO* deletion mutant, and complemented *ndhO* strains in air.

Supplemental Table S1. Primer list and sequences.

Received March 20, 2016; accepted April 15, 2016; published April 20, 2016.

LITERATURE CITED

Allen MM (1968) Simple conditions for growth of unicellular blue-green algae on plates. J Phycol **4:** 1–4

Arteni AA, Zhang P, Battchikova N, Ogawa T, Aro E-M, Boekema EJ (2006) Structural characterization of NDH-1 complexes of *Thermosynechococcus elongatus* by single particle electron microscopy. Biochim Biophys Acta **1757:** 1469–1475

Baradaran R, Berrisford JM, Minhas GS, Sazanov LA (2013) Crystal structure of the entire respiratory complex I. Nature **494:** 443–448

Battchikova N, Eisenhut M, Aro E-M (2011a) Cyanobacterial NDH-1 complexes: novel insights and remaining puzzles. Biochim Biophys Acta **1807:** 935–944

Battchikova N, Wei L, Du L, Bersanini L, Aro E-M, Ma W (2011b) Identification of novel Ssl0352 protein (NdhS), essential for efficient operation of cyclic electron transport around photosystem I, in NADPH:plastoquinone oxidoreductase (NDH-1) complexes of *Synechocystis* sp. PCC 6803. J Biol Chem **286:** 36992–37001

Battchikova N, Zhang P, Rudd S, Ogawa T, Aro E-M (2005) Identification of NdhL and Ssl1690 (NdhO) in NDH-1L and NDH-1M complexes of *Synechocystis* sp. PCC 6803. J Biol Chem **280:** 2587–2595

Berger S, Ellersiek U, Steinmüller K (1991) Cyanobacteria contain a mitochondrial complex I-homologous NADH-dehydrogenase. FEBS Lett **286:** 129–132

Birungi M, Folea M, Battchikova N, Xu M, Mi H, Ogawa T, Aro E-M, Boekema EJ (2010) Possibilities of subunit localization with fluorescent protein tags and electron microscopy examplified by a cyanobacterial NDH-1 study. Biochim Biophys Acta **1797:** 1681–1686

Dai H, Zhang L, Zhang J, Mi H, Ogawa T, Ma W (2013) Identification of a cyanobacterial CRR6 protein, Slr1097, required for efficient assembly of NDH-1 complexes in *Synechocystis* sp. PCC 6803. Plant J **75:** 858–866

Deng Y, Ye J, Mi H (2003) Effects of low CO_2 on NAD(P)H dehydrogenase, a mediator of cyclic electron transport around photosystem I in the cyanobacterium *synechocystis* PCC6803. Plant Cell Physiol **44:** 534–540

Dworsky A, Mayer B, Regelsberger G, Fromwald S, Peschek GA (1995) Functional and immunological characterization of both "mitochondria-like" and "chloroplast-like" electron/proton transport proteins in isolated and purified cyanobacterial membranes. Bioelectrochem Bioenerg **38:** 35–43

Folea IM, Zhang P, Nowaczyk MM, Ogawa T, Aro E-M, Boekema EJ (2008) Single particle analysis of thylakoid proteins from *Thermosynechococcus elongatus* and *Synechocystis* 6803: localization of the CupA subunit of NDH-1. FEBS Lett **582:** 249–254

Friedrich T, Scheide D (2000) The respiratory complex I of bacteria, archaea and eukarya and its module common with membrane-bound multisubunit hydrogenases. FEBS Lett **479:** 1–5

Friedrich T, Steinmüller K, Weiss H (1995) The proton-pumping respiratory complex I of bacteria and mitochondria and its homologue in chloroplasts. FEBS Lett **367:** 107–111

Gao F, Zhao J, Wang X, Qin S, Wei L, Ma W (2016) NdhV is a subunit of NADPH dehydrogenase essential for cyclic electron transport in *Synechocystis* sp. strain PCC 6803. Plant Physiol **170:** 752–760

Gombos Z, Wada H, Murata N (1994) The recovery of photosynthesis from low-temperature photoinhibition is accelerated by the unsaturation of membrane lipids: a mechanism of chilling tolerance. Proc Natl Acad Sci USA **91:** 8787–8791

He Z, Xu M, Wu Y, Lv J, Fu P, Mi H (2016) NdhM subunit is required for the stability and the function of NAD(P)H dehydrogenase complexes involved in CO_2 uptake in *Synechocystis* sp. strain PCC 6803. J Biol Chem **291:** 5902–5912

He Z, Zheng F, Wu Y, Li Q, Lv J, Fu P, Mi H (2015) NDH-1L interacts with ferredoxin via the subunit NdhS in *Thermosynechococcus elongatus*. Photosynth Res **126:** 341–349

Herranen M, Battchikova N, Zhang P, Graf A, Sirpiö S, Paakkarinen V, Aro E-M (2004) Towards functional proteomics of membrane protein complexes in *Synechocystis* sp. PCC 6803. Plant Physiol **134:** 470–481

Ifuku K, Endo T, Shikanai T, Aro E-M (2011) Structure of the chloroplast NADH dehydrogenase-like complex: nomenclature for nuclear-encoded subunits. Plant Cell Physiol **52:** 1560–1568

Klughammer B, Sültemeyer D, Badger MR, Price GD (1999) The involvement of NAD(P)H dehydrogenase subunits, NdhD3 and NdhF3, in high-affinity CO_2 uptake in *Synechococcus* sp. PCC7002 gives evidence for multiple NDH-1 complexes with specific roles in cyanobacteria. Mol Microbiol **32:** 1305–1315

Kubota H, Sakurai I, Katayama K, Mizusawa N, Ohashi S, Kobayashi M, Zhang P, Aro E-M, Wada H (2010) Purification and characterization of photosystem I complex from *Synechocystis* sp. PCC 6803 by expressing histidine-tagged subunits. Biochim Biophys Acta **1797:** 98–105

Kügler M, Jänsch L, Kruft V, Schmitz U, Braun HP (1997) Analysis of the chloroplast protein complexes by blue-native polyacrylamide gel electrophoresis (BN-PAGE). Photosynth Res **53:** 35–44

Laemmli UK (1970) Cleavage of structural proteins during the assembly of the head of bacteriophage T4. Nature **227:** 680–685

Lagarde D, Beuf L, Vermaas W (2000) Increased production of zeaxanthin and other pigments by application of genetic engineering techniques to *Synechocystis* sp. strain PCC 6803. Appl Environ Microbiol **66:** 64–72

Ma W, Ogawa T (2015) Oxygenic photosynthesis-specific subunits of cyanobacterial NADPH dehydrogenases. IUBMB Life **67:** 3–8

Maeda S, Badger MR, Price GD (2002) Novel gene products associated with NdhD3/D4-containing NDH-1 complexes are involved in photosynthetic CO_2 hydration in the cyanobacterium, *Synechococcus* sp. PCC7942. Mol Microbiol **43:** 425–435

Mi H, Endo T, Ogawa T, Asada K (1995) Thylakoid membrane-bound, NADPH-specific pyridine nucleotide dehydrogenase complex mediates cyclic electron transport in the cyanobacterium *Synechocystis* sp. PCC 6803. Plant Cell Physiol **36:** 661–668

Mi H, Endo T, Schreiber U, Ogawa T, Asada K (1992) Electron donation from cyclic and respiratory flows to the photosynthetic intersystem chain is mediated by pyridine nucleotide dehydrogenase in the cyanobacterium *Synechocystis* PCC 6803. Plant Cell Physiol **33:** 1233–1237

Munekage Y, Hashimoto M, Miyake C, Tomizawa K, Endo T, Tasaka M, Shikanai T (2004) Cyclic electron flow around photosystem I is essential for photosynthesis. Nature **429:** 579–582

Nowaczyk MM, Wulfhorst H, Ryan CM, Souda P, Zhang H, Cramer WA, Whitelegge JP (2011) NdhP and NdhQ: two novel small subunits of the cyanobacterial NDH-1 complex. Biochemistry **50:** 1121–1124

Ogawa T (1991) A gene homologous to the subunit-2 gene of NADH dehydrogenase is essential to inorganic carbon transport of *Synechocystis* PCC6803. Proc Natl Acad Sci USA **88:** 4275–4279

Ogawa T, Mi H (2007) Cyanobacterial NADPH dehydrogenase complexes. Photosynth Res **93:** 69–77

Ohkawa H, Pakrasi HB, Ogawa T (2000) Two types of functionally distinct NAD(P)H dehydrogenases in *Synechocystis* sp. strain PCC6803. J Biol Chem **275:** 31630–31634

Peltier G, Cournac L (2002) Chlororespiration. Annu Rev Plant Biol **53:** 523–550

Peng L, Fukao Y, Fujiwara M, Shikanai T (2012) Multistep assembly of chloroplast NADH dehydrogenase-like subcomplex A requires several nucleus-encoded proteins, including CRR41 and CRR42, in Arabidopsis. Plant Cell **24:** 202–214

Peng L, Fukao Y, Fujiwara M, Takami T, Shikanai T (2009) Efficient operation of NAD(P)H dehydrogenase requires supercomplex formation with photosystem I via minor LHCI in Arabidopsis. Plant Cell **21:** 3623–3640

Peng L, Fukao Y, Myouga F, Motohashi R, Shinozaki K, Shikanai T (2011) A chaperonin subunit with unique structures is essential for folding of a specific substrate. PLoS Biol **9:** e1001040

Pieulle L, Guedeney G, Cassier-Chauvat C, Jeanjean R, Chauvat F, Peltier G (2000) The gene encoding the NdhH subunit of type 1 NAD(P)H dehydrogenase is essential to survival of *Synechocystis* PCC6803. FEBS Lett **487:** 272–276

Prommeenate P, Lennon AM, Markert C, Hippler M, Nixon PJ (2004) Subunit composition of NDH-1 complexes of *Synechocystis* sp. PCC 6803: identification of two new *ndh* gene products with nuclear-encoded homologues in the chloroplast Ndh complex. J Biol Chem **279:** 28165–28173

Rumeau D, Bécuwe-Linka N, Beyly A, Louwagie M, Garin J, Peltier G (2005) New subunits NDH-M, -N, and -O, encoded by nuclear genes, are essential for plastid Ndh complex functioning in higher plants. Plant Cell **17:** 219–232

Sazanov LA, Hinchliffe P (2006) Structure of the hydrophilic domain of respiratory complex I from *Thermus thermophilus*. Science **311:** 1430–1436

Schwarz D, Schubert H, Georg J, Hess WR, Hagemann M (2013) The gene *sml0013* of *Synechocystis* species strain PCC 6803 encodes for a novel subunit of the NAD(P)H oxidoreductase or complex I that is ubiquitously distributed among cyanobacteria. Plant Physiol **163:** 1191–1202

Shibata M, Ohkawa H, Kaneko T, Fukuzawa H, Tabata S, Kaplan A, Ogawa T (2001) Distinct constitutive and low-CO_2-induced CO_2 uptake systems in cyanobacteria: genes involved and their phylogenetic relationship with homologous genes in other organisms. Proc Natl Acad Sci USA **98:** 11789–11794

Shimizu H, Peng L, Myouga F, Motohashi R, Shinozaki K, Shikanai T (2008) CRR23/NdhL is a subunit of the chloroplast NAD(P)H dehydrogenase complex in Arabidopsis. Plant Cell Physiol **49:** 835–842

Vinothkumar KR, Zhu J, Hirst J (2014) Architecture of mammalian respiratory complex I. Nature **515:** 80–84

Williams JGK, Szalay AA (1983) Stable integration of foreign DNA into the chromosome of the cyanobacterium *Synechococcus* R2. Gene **24:** 37–51

Wu Y, Zheng F, Ma W, Han Z, Gu Q, Shen Y, Mi H (2011) Regulation of NAD(P)H dehydrogenase-dependent cyclic electron transport around PSI by $NaHSO_3$ at low concentrations in tobacco chloroplasts. Plant Cell Physiol **52:** 1734–1743

Wulfhorst H, Franken LE, Wessinghage T, Boekema EJ, Nowaczyk MM (2014) The 5 kDa protein NdhP is essential for stable NDH-1L assembly in *Thermosynechococcus elongatus*. PLoS One **9:** e103584

Xu M, Ogawa T, Pakrasi HB, Mi H (2008) Identification and localization of the CupB protein involved in constitutive CO_2 uptake in the cyanobacterium, *Synechocystis* sp. strain PCC 6803. Plant Cell Physiol **49:** 994–997

Yamamoto H, Peng L, Fukao Y, Shikanai T (2011) An Src homology 3 domain-like fold protein forms a ferredoxin binding site for the chloroplast NADH dehydrogenase-like complex in Arabidopsis. Plant Cell **23:** 1480–1493

Yamamoto H, Shikanai T (2013) In *planta* mutagenesis of Src homology 3 domain-like fold of NdhS, a ferredoxin-binding subunit of the chloroplast NADH dehydrogenase-like complex in Arabidopsis: a conserved Arg-193 plays a critical role in ferredoxin binding. J Biol Chem **288:** 36328–36337

Zhang J, Gao F, Zhao J, Ogawa T, Wang Q, Ma W (2014) NdhP is an exclusive subunit of large complex of NADPH dehydrogenase essential to stabilize the complex in *Synechocystis* sp. strain PCC 6803. J Biol Chem **289:** 18770–18781

Zhang P, Battchikova N, Jansen T, Appel J, Ogawa T, Aro E-M (2004) Expression and functional roles of the two distinct NDH-1 complexes and the carbon acquisition complex NdhD3/NdhF3/CupA/Sll1735 in *Synechocystis* sp PCC 6803. Plant Cell **16:** 3326–3340

Zhang P, Battchikova N, Paakkarinen V, Katoh H, Iwai M, Ikeuchi M, Pakrasi HB, Ogawa T, Aro E-M (2005) Isolation, subunit composition and interaction of the NDH-1 complexes from *Thermosynechococcus elongatus* BP-1. Biochem J **390:** 513–520

Zhao J, Gao F, Zhang J, Ogawa T, Ma W (2014) NdhO, a subunit of NADPH dehydrogenase, destabilizes medium size complex of the enzyme in *Synechocystis* sp. strain PCC 6803. J Biol Chem **289:** 26669–26676

Zhao J, Rong W, Gao F, Ogawa T, Ma W (2015) Subunit Q is required to stabilize the large complex of NADPH dehydrogenase in *Synechocystis* sp. strain PCC 6803. Plant Physiol **168:** 443–451

Zickermann V, Wirth C, Nasiri H, Siegmund K, Schwalbe H, Hunte C, Brandt U (2015) Structural biology. Mechanistic insight from the crystal structure of mitochondrial complex I. Science **347:** 44–49